Isothermal-Crystallization Kinetics and Melting Behavior of Crystalline/Crystalline Blends of Poly(trimethylene terephthalate) and Poly(ethylene 2,6-naphthalate)

Mingtao Run, Yingjin Wang, Chenguang Yao, Hongchi Zhao

College of Chemistry and Environmental Science, Hebei University, Baoding 071002, China

Received 1 June 2006; accepted 8 August 2006
DOI 10.1002/app.25254
Published online in Wiley InterScience (www.interscience.wiley.com).

ABSTRACT: The isothermal crystallization and crystal morphology of poly(trimethylene terephthalate) (PTT)/poly (ethylene 2,6-naphthalate) (PEN) blends were investigated with differential scanning calorimetry and polarized optical microscopy. The commonly used Avrami equation was used to fit the primary stage of isothermal crystallization. The Avrami exponents were evaluated to be in the range of 3.0–3.3 for isothermal crystallization. The subsequent melting endotherms of the blends after isothermal crystallization showed multiple melting peaks. The crystallization activation energies of the blends with 20 or 40% PTT was −48.3 and −60.9 kJ/mol, respectively, as calculated by the Arrhenius formula for the isothermal-crystallization processes. The Hoffman–Lauritzen theory was also employed to fit the process of isothermal crystallization, and the kinetic parameters of the blends with 20 or 40% PTT were determined to be 1.5×10^5 and 1.8×10^5 K^2, respectively. The spherulite morphology of the six binary blends formed at 190°C showed different sizes and perfect Maltese crosses when the PTT or PEN component was varied, suggesting that the greater the PTT content was, the larger or more perfect the crystallites were that formed in the binary blends. J Appl Polym Sci 103: 3316–3325, 2007

Key words: activation energy; blends; calorimetry; compatibility; crystallization

INTRODUCTION

Poly(trimethylene terephthalate) (PTT) was first patented by Whinfield and Dickson[1] in 1946 and commercially produced by Shell Chemicals until the 1990s. Many properties of PTT are between those of poly(ethylene terephthalate) (PET) and poly(butylene terephthalate) (PBT), such as the crystallization rate and glass-transition temperature (T_g). Moreover, it combines the two key advantages of PET and PBT into one polymer, and it has important applications in the textile industry[2] and is a promising engineering thermoplastic.[3] Poly(ethylene 2,6-naphthalate) (PEN), featuring a molecular structure of a naphthalene ring instead of the benzene ring in PET, is used as a high-performance polymer and has superior strength, heat stability, and barrier properties because of its increased chain stiffness.[4] Thus, PEN is used in a variety of applications, such as tire cords for automobiles[5] and base films for videotapes.[6–8]

Polymer blending is an attractive alternative for producing new polymeric materials with desirable properties without the synthesis of a totally new material. Other advantages of polymer blending are versatility, simplicity, and low cost. Because of the similarity of the chemical structures of these linear aromatic polyesters, numerous research works related to various aspects of polyester blends are available in the reported literature. Blends of polyesters have been investigated widely, such as PEN and poly(butylene 2,6-naphthalate),[9] PET and PBT,[10] PET and PEN,[11] PTT and PET,[12] PTT and PBT,[13] and PTT and PEN.[14] To meet the growing demands for new materials, the combination of different polyesters, such as blends of PTT and PEN, may be very important for making economic and advanced materials.[15]

Recently, Krutphun and Supaphol[14] studied the miscibility, melting, and crystallization behavior of PTT/PEN blends. Their PTT/PEN blends were miscible in the amorphous state in all the blend compositions studied, as evidenced by a single, composition-dependent T_g observed for each blend composition. The variation in the T_g value with the blend composition was well predicted by the Gordon–Taylor equation, with the fitting parameter being 0.57. The cold-crystallization peak temperature (T_{cc}) decreased with increasing PTT content, whereas the melt-crystallization peak temperature decreased with an increasing amount of the minor component. The subsequent melting behavior after both cold and melt crystallization exhibited melting point depression, in which the observed melting temperatures (T_m's) decreased with an increasing amount of the minor component. During melt crystallization, both components in the blends

Correspondence to: M. Run (rmthyp@hotmail.com).

crystallized concurrently just to form their own crystals. The blend with 60% (w/w) PTT exhibited the lowest total apparent degree of crystallinity.

Studies related to the kinetics of polymer crystallization are of great importance in polymer processing because the resulting physical properties are strongly dependent on the morphology formed and the extent of crystallization occurring during processing. In this study, blends of PTT and PEN were prepared and characterized for their isothermal-crystallization kinetics and subsequent melting behavior with differential scanning calorimetry (DSC) measurements. The objectives of this work were (1) to investigate the effect of the blend composition on the melt-crystallization behavior, (2) to investigate the effect of the blend composition on the isothermal-crystallization kinetics, and (3) to the assess the effect of the blend composition on the crystal morphology of the binary blend.

EXPERIMENTAL

Materials

The PTT homopolymer was supplied in pellet form (Montreal PTT PolyCanad LP, Montreal, Canada) with an intrinsic viscosity of 0.92 dL/g measured in a phenol/tetrachloroethane solution (50/50 w/w) at 25°C. The PEN homopolymer was supplied in pellet form (HoneyWell Co., USA) with an intrinsic viscosity of 0.89 dL/g measured in a phenol/tetrachloroethane solution (60/40 w/w) at 30°C.

Blend preparation

The materials were dried in a vacuum oven at 120°C for 12 h before the blends were prepared. The dried pellets of PTT and PEN were mixed together with different weight ratios of PTT to PEN as follows: B1, 0/100; B2, 20/80; B3, 40/60; B4, 60/40; B5, 80/20; and B6, 100/0. Then, they were melt-blended in a ZSK-25WLE (WP Co., Germany) self-wiping, corotating, twin-screw extruder operating at a screw speed of 60 rpm and at a die temperature of 300°C. The resultant blend ribbons were quenched, cut up, and redried before being used in DSC.

DSC

The T_g, cold-crystallization behavior, subsequent melting behavior, and melt-crystallization behavior of six samples were studied with a PerkinElmer Diamond DSC (Perkin-Elmer Co., Shelton, CT) instrument that was calibrated with indium before the measurements were performed, and the weights of all samples were approximately 6.0 mg. The samples were heated to 300°C at 100°C/min under a nitrogen atmosphere and held for 5 min to reset previous thermal histories; after this, all the samples were immediately quenched at a cooling rate of 200°C/min to obtain a completely amorphous state and then heated to 300°C at a heating rate of 10°C/min. Then, the melt was held for 5 min and subsequently cooled to 50°C at a constant cooling rate of 10°C/min. The final melting and cooling processes were recorded.

The isothermal crystallization and subsequent melting behaviors of two selected blends (B2 and B3) were performed as follows: the samples were heated to 300°C at 100°C/min under a nitrogen atmosphere, held for 5 min, and then cooled at 200°C/min to the designated crystallization temperature (T_c) rapidly; after the isothermal crystallization was finished, the samples were heated to 300°C at a rate of 10°C/min. The exothermic curves of the heat flow as a function of time were recorded and investigated. A sample cut from one sheet was used only once, and its weight was around 6 ± 0.5 mg.

Polarized optical microscopy (POM)

The crystal morphology of PTT/PEN was studied with a Leitz SM-LUX-POL polarized optical microscope (SM-LUX-POL, Leitz, Germany) equipped with a hot stage and a camera system. We prepared the sample by sandwiching a tiny pellet of the blend ribbon between two glass plates at a distance of about 200 μm, compressing it at 300°C for 5 min in an oven, and then placing it on a hot stage at 190°C; we then took photographs with a camera.

RESULTS AND DISCUSSION

T_g, cold-crystallization, and melting behavior

Generally, a single T_g or its shift in blends represents miscibility or partial miscibility.[16–18] In our experiments, all the blends were thought to be miscible in the amorphous phase. This was in good agreement with the report of Krutphun and Supaphol.[14] Figure 1 displays the DSC curves of the glass transition, cold crystallization, and subsequent melting for six quenched samples recorded at a heating rate of 10°C/min, and the parameters are listed in Table I. Figure 1 shows the dependence of T_g on the blend composition. A single T_g can be observed in each curve, and the T_g values of the B2–B5 blends can be observed between those of the pure components (T_g for PTT = 46.2°C, T_g for PEN = 125.9°C). T_g of each blend shifts to a higher temperature with an increasing concentration of PEN, although their transitions are not as sharp as that of the pure polymer. This result suggests that PTT and PEN are completely miscible in the amorphous phase for all blend compositions, whereas the T_g range is wider in DSC curves for B2–B5 blends than that of the glass transition of the two pure polymers. Shi and Jabarin[19]

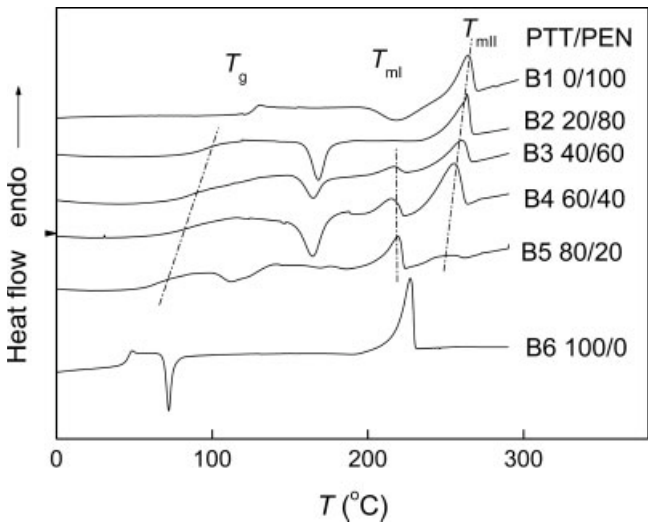

Figure 1 T_g, cold-crystallization, and subsequent melting thermograms of six samples at a heating rate of 10°C/min.

reported the glass transition of a blend of PET and PEN, and only one T_g was observed in each blend curve. The reason is that some compatibilization occurred as a result of the formation of PET and PEN copolymers during the process, and thus the blends became sufficiently compatible; DSC was not sensitive enough to detect phase separation or the existence of two T_g's. In this work, T_g also increased linearly with the blend composition, indicating that the blend system was a miscible and stable mixture.

The cold-crystallization behaviors of the six samples are also shown in Figure 1. According to Figure 1 and Table I, T_{cc} of pure PTT (B6) is about 72.0°C, which is in good agreement with an earlier observed value of 70°C.[11] However, T_{cc} for pure PEN (B1) can be observed at about 219.3°C in the DSC curve, which suggests that PEN cannot crystallize at a low temperature at a heating rate of 10°C/min because of its chain stiffness. Apparently, each of the blends from B2 to B5 shows a single, component-dependent T_{cc}, and the T_{cc} values decrease from 168.3 to 112.9°C. The cold-crystallization peaks of B2, B3, and B4 show almost the same T_c values of 168.3, 165.0, and 164.6°C. These values are much smaller than T_{cc} of B1 (PEN) because of the dilution effect of PTT. These cold-crystallization peaks should predominantly correspond to the cold-crystallization behavior of the PEN component because of the high T_{cc} values, but the cold-crystallization behavior of the PTT component cannot be observed in these DSC curves. On the other hand, the cold-crystallization peak of B5 (PTT80/PEN20) can be predominantly attributed to the cold crystallization of major component PTT because of its low temperature, whereas the cold crystallization of the PEN component cannot be detected clearly. These results suggest that in the PTT range of 20–60%, the PEN molecules can crystallize only at a higher temperature above 140°C because of its stiff molecular chains. However, by careful observation, we can find that the starting temperature of the cold crystallization of B2, B3, and B4 decreases with an increasing concentration of PTT.

As shown in Figure 1, the subsequent melting behaviors for the six samples after cold crystallization are different as the blend component varies. Obviously, the DSC curves of the PTT (B6) and PEN (B1) blends show a single melting peak (T_m), and their T_m values are 227.1 and 264.0°C, respectively. The curves of the B3, B4, and B5 blends exhibit double melting peaks, and the value of T_m decreases gradually with an increasing amount of the minor component, whereas melting peak T_{mI} of B2 cannot be detected in the DSC curve.

Melt-crystallization behavior

Figure 2 shows the DSC curves of the six samples with various PTT contents at a given cooling rate, and the crystallization parameters are listed in Table I. According to Figure 2 and Table I, an apparent exotherm can be observed for PTT with a crystallization peak temperature (T_p) of 186.7°C, whereas no crystallization isotherms but only a glass transition at about 122.5°C of pure PEN can be seen at the same cooling rate of 10°C/min. These results suggest that PTT with flexible molecular chains is more crystallizable than PEN with stiff chains, and the crystallization for PEN is almost inhibited at this cooling rate.

For the B2 and B3 blends, each curve is shown with only one crystallization exothermic peak at a higher temperature (211.6 and 208.3°C, respectively), indicating that the molecular chains of PEN can crystallize at

TABLE I
DSC Parameters of the Six Samples

	Melting process				Melt-crystallization process				
Sample	T_g (°C)	T_{cc} (°C)	T_{mI} (°C)	T_{mII} (°C)	T_{onset} (°C)	T_{pI} (°C)	ΔH_{cI} (J/g)	T_{pII} (°C)	ΔH_{cII} (J/g)
B1	125.9	219.3	—	264.0	—	—	—	—	0
B2	97.6	168.3	—	260.4	220.6	—	—	211.6	−59.3
B3	91.1	165.0	215.5	263.8	215.6	—	—	208.3	−32.9
B4	83.8	164.6	214.7	255.4	213.9	162.0	−10.0	204.6	−23.7
B5	68.5	112.9	219.8	252.0	206.6	148.3	−34.9	201.4	−5.4
B6	46.2	72.0	227.1	—	186.7	176.7	−50.5	—	—

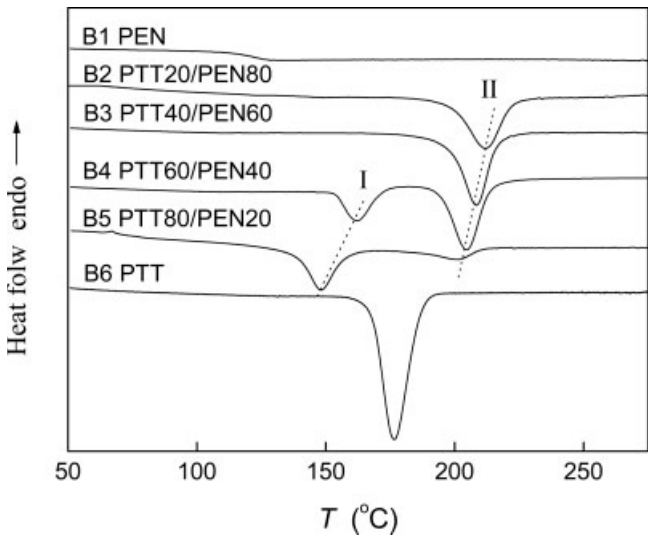

Figure 2 DSC melt-crystallization curves of six samples at a cooling rate of 10°C/min.

a cooling rate of 10°C/min with PTT in the blend melt. However, no exothermic peak can be observed at a lower temperature that may correspond to the crystallization of PTT in the DSC curve, and this suggests that the crystallization behavior of the PTT component is inhibited by the major component (PEN), although the weight percentage of PTT is 20% in B2 and 40% in B3. In these two binary blends, the PTT component may be a plasticizer that dilutes the concentration of PEN and improves the arrangement behavior of PEN molecular chains; as a result, the crystallization of PEN starts at a higher temperature.

During the melt crystallization of the polymers, the crystallization enthalpy (ΔH_c) was recorded by DSC from the start to the end of crystallization, and this suggests the crystallization extent of a specific polymer; that is, the larger ΔH_c is, the more crystals are formed in the polymer. The values of $\Delta H_{c\mathrm{II}}$ for B1 and B2 increase from 0 to −59.3 J/g, and this strongly supports the supposition that the PTT component plays the role of a plasticizer and improves the crystallization ability of the PEN component. Moreover, the values of $\Delta H_{c\mathrm{II}}$ decrease gradually from −59.3 (B2) to −5.4 J/g (B5), and $\Delta H_{c\mathrm{I}}$ increases gradually from −10.0 (B4) to −50.5 J/g (B6), corresponding to the contents in the blends.

However, the exotherms of the B4 and B5 blends exhibit two main crystallization peaks: peak II at a higher temperature and peak I at a lower temperature. This may be attributed to the crystallizations of PEN and PTT, respectively. The results suggest that both the PTT and PEN components in the blends crystallize individually when PTT becomes the major component. By careful observation, we have found that the $T_{p\mathrm{II}}$ values of the PEN component in the blends decrease monotonically with a decreasing amount of the PEN component, suggesting that the crystallization behavior of the PEN component in the blends is relevant to its amount. On the other hand, the $T_{p\mathrm{I}}$ values of B4 and B5 are lower than that of pure PTT, suggesting that the crystallization of the PTT component may be retarded by the PEN crystals that have formed at higher temperatures.[14] Interestingly, $T_{p\mathrm{I}}$ of B4 is higher than that of B5, and this suggests that the PEN crystals already present in the system may act as nucleating substrates to a certain extent for the crystal growth of PTT.

Isothermal-crystallization kinetic analysis

Isothermal-crystallization behavior

The relative crystallinity at time t (X_t) is defined by the following equation:

$$X_t = \frac{\int_{t_0}^{t} (dH/dt)dt}{\int_{t_0}^{t_\infty} (dH/dt)dt} \quad (1)$$

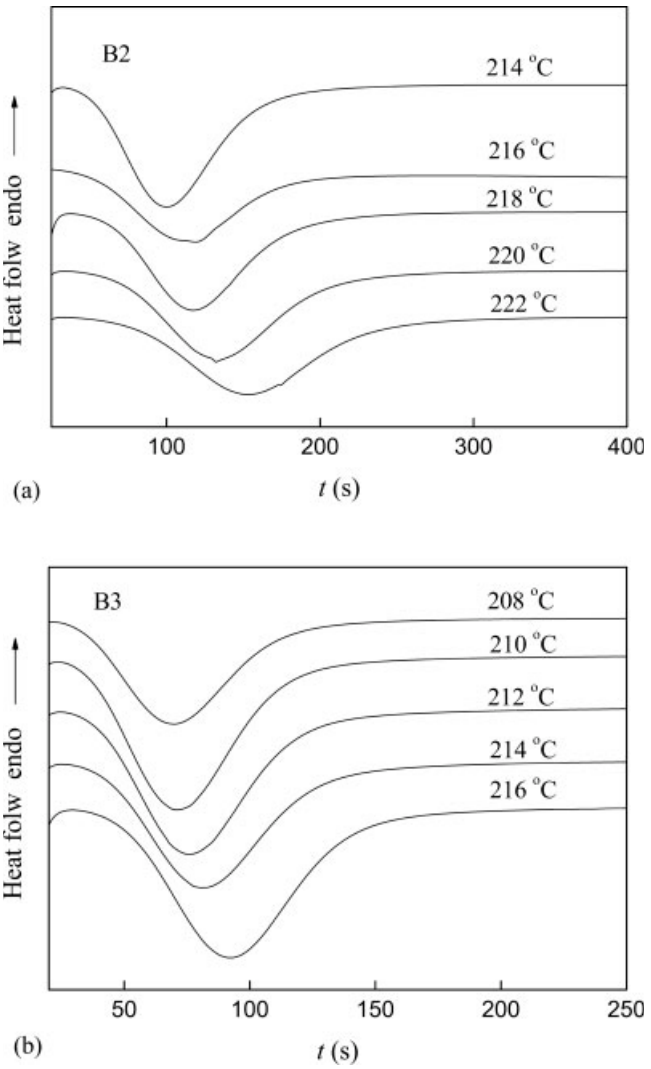

Figure 3 DSC thermograms of (a) B2 and (b) B3 blends during isothermal crystallization at different designated temperatures.

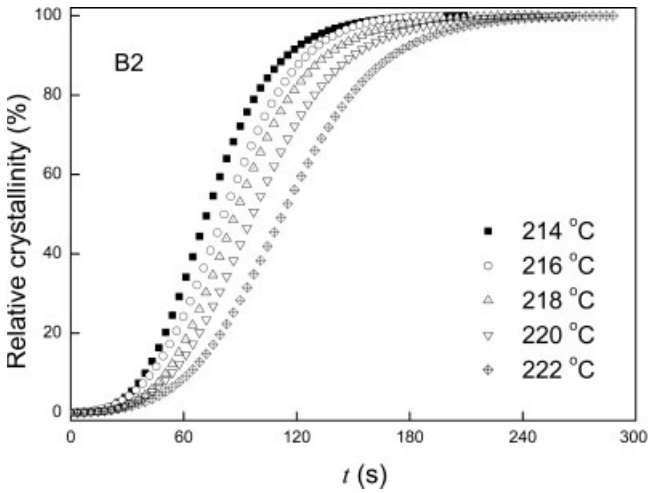

Figure 4 Development of X_t with t for the isothermal crystallization of B2 blend at different designated temperatures.

where dH/dt is the rate of heat evolution and t_0 and t_∞ are the times at which crystallization starts and ends, respectively.

For the complicated crystallization behavior of the B4 (PTT60/PEN40) and B5 (PTT80/PEN20) blends, it is difficult to study their crystallization kinetics. In this section, only the B2 (PTT20/PEN80) and B3 (PTT40/PEN60) blends have been selected to investigate the isothermal-crystallization behavior because of their regular crystallization peaks in the crystallization curves, and the influence of PTT on the isothermal-crystallization behavior and kinetics of PEN is considered. As shown in Figure 3(a,b), the isothermal crystallization of the B2 and B3 blends has been carried out at five designated temperatures. From the exotherms in Figure 3, it can be easily found that each of the DSC curves displays only one exothermic peak at each designated temperature.

Generally, the isothermal-crystallization kinetics of different samples should be discussed under the same T_c from 208 to 222°C. However, it is difficult to obtain the exothermal curves for B3 at temperatures up to 218°C because of the experimental limitation that T_c is usually determined by the onset temperature (T_{onset}). Therefore, T_c of B3 has been selected in a temperature range of 208–216°C, which is lower than that of B2 (214–222°C). Meanwhile, the common T_c value (e.g., 214 or 216°C) has been selected as much as we can to compare the differences for the crystallization kinetics.

As shown in Figure 3, with T_c increasing, the exothermic peak of each curve is shifted to a longer time. Figure 4 shows X_t integrated from Figure 3(a) as a function of the crystallization time (t) at various T_c values; the characteristic sigmoidal isotherms are shifted right along the time axis with increasing T_c, and the whole crystallization time (t_c) increases with T_c (Table II). Similar curves have been obtained for B2 and B3.

To compare the crystallization rates at various temperatures, the half-time of crystallization ($t_{1/2}$) is listed in Table II. The crystallization rate can be qualitatively compared by the value of $t_{1/2}$. $t_{1/2}$ is enhanced greatly with an increase of T_c, and this indicates that the crystallization rates of the binary blend decrease with increasing T_c. Moreover, a comparison of the values of $t_{1/2}$ for B2 and B3 at the same temperatures (214 and 216°C) shows that the results for B3 are lower than those for B2, indicating that the greater the PTT content is, the higher the crystallization rate is.

Isothermal-crystallization analysis based on the Avrami equation

Assuming that X_t increases with t, we can used the Avrami equation to analyze the isothermal-crystallization process of PTT/PEN as follows:[20,21]

$$1 - X_t = \exp(-K_t t^n) \tag{2}$$

$$\log[-\ln(1 - X_t)] = n \log t + \log K_t \tag{3}$$

where Avrami exponent n is a mechanism constant with a value depending on the type of nucleation and the growth dimension and crystallization rate parameter K_t is a growth rate constant involving both nucleation and growth rate parameters.

Plots of $\log[-\ln(1 - X_t)]$ versus $\log t$ according to eq. (3) are shown in Figure 5(a,b), and each curve is composed of two linear sections. This fact indicates the crystallization process is composed of primary and secondary crystallization stages. During the latter

TABLE II
Isothermal Crystallization Kinetic Parameters Analyzed with the Avrami Equation

B2					B3				
T (°C)	t_c (s)	$t_{1/2}$ (s)	n	K_t (10^{-7} s^{-n})	T (°C)	t_c (s)	$t_{1/2}$ (s)	n	K_t (10^{-7} s^{-n})
214	208.8	72	3.1	9.7	208	148.9	48	3.0	43.8
216	226.6	81	3.0	6.8	210	164.4	50	3.0	45.2
218	249.5	88	3.2	3.7	212	196.0	53	3.1	23.2
220	268.8	97	3.3	3.0	214	226.0	60	3.2	11.3
222	290.0	113	3.3	1.9	216	241.2	65	3.2	9.5

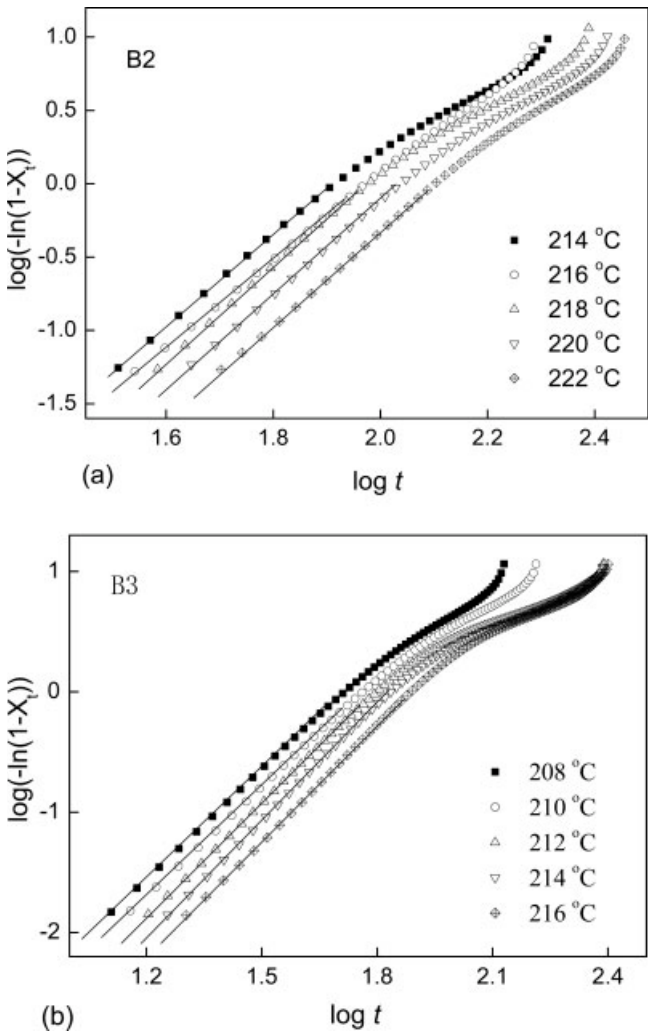

Figure 5 Plots of $\log[-\ln(1 - X_t)]$ versus $\log t$ for the isothermal crystallization of (a) B2 and (b) B3 blends.

stage, the crystallization of chain segments occurs between the crystalline structures already formed and the crystallization of the amorphous, intercrystalline areas.[22–24]

n and K_t can be readily extracted from the primary stage plots in Figure 5, and their values at various designated temperatures are listed in Table II. In this work, the values of n are between 3.0 and 3.3 for both B2 and B3, which may be average values of complex nucleating types and growth dimensions of crystals occurring simultaneously in the crystallization process. n in the range of 3.0–3.3 indicates a three-dimensional growth mechanism with a combination of thermal and athermal nucleation (resulting in the fractional n values observed).[25,26] With increasing temperature, the values of n increase gradually from 3.1 to 3.3 for B2 and from 3.0 to 3.2 for B3. The temperature dependence of n, within the nucleation-controlled region, should be such that n increases with increasing T_c. This may be explained by the fact that the number of thermal nuclei increases tremendously as the temperature increases.[27,28] In other words, as T_c increases, the number of thermal nuclei that become stable at that temperature also increases, and this causes n to increase.

The K_t values of the B2 and B3 blends at various designated temperatures are listed in Table II and compared; the values of K_t gradually decrease with increasing T_c. This suggests that in the isothermal-crystallization process, the higher T_c is, the lower the crystallization rate is. Furthermore, a comparison of the values of K_t at the same T_c values shows that the results for B2 are lower than those for B3, and this is confirmed by the conclusion of $t_{1/2}$.

Melting behavior of the binary blends

Figure 6 shows the DSC heating scans of B2 and B3 blends at a heating rate of 10°C/min after the comple-

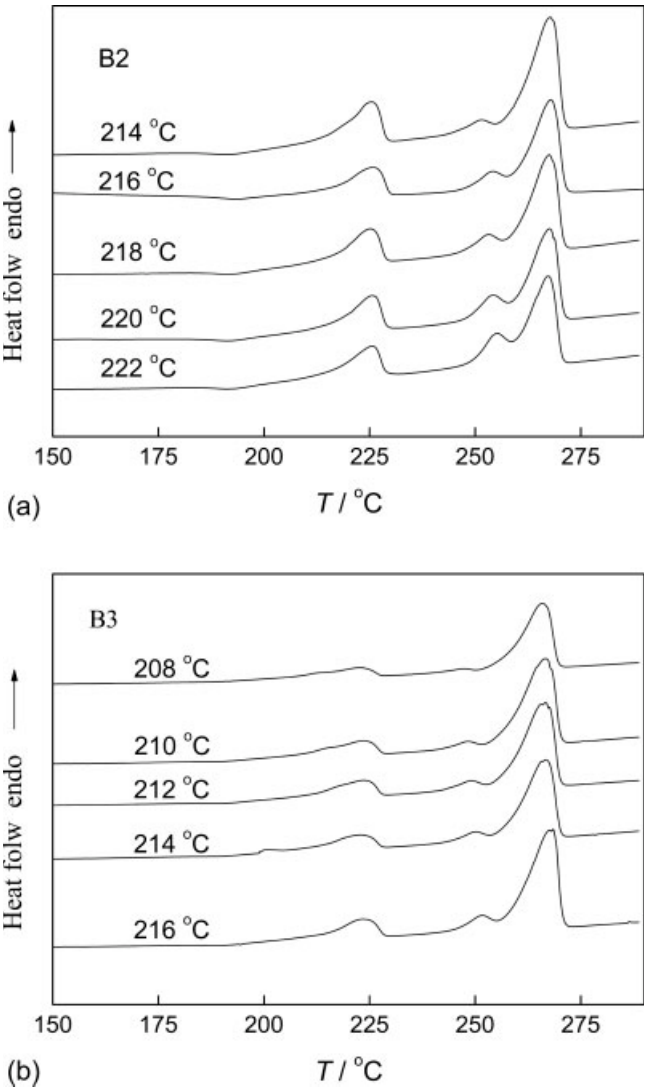

Figure 6 Melting endotherms of (a) B2 and (b) B3 blends at a heating rate of 10°C/min after isothermal crystallization at the specified temperatures.

TABLE III
Melting Endotherm Parameters of B2 and B3

Sample	T_c (°C)	T_{mI} (°C)	$\Delta H_{f(I)}$ (J/g)	T_{mII} (°C)	T_{mIII} (°C)	$\Delta H_{f(II+III)}$ (J/g)
B2	214	225.3	−12.6	251.8	267.6	−31.9
	216	225.6	−13.1	253.3	267.8	−31.8
	218	225.3	−13.7	253.3	267.7	−32.2
	220	225.6	−13.3	254.3	267.7	−32.4
	222	225.7	−12.9	255.0	267.6	−32.8
B3	208	223.4	−8.6	248.1	265.8	−36.0
	210	224.2	−8.9	248.5	266.5	−36.3
	212	224.2	−9.4	249.2	266.5	−35.8
	214	224.2	−8.5	250.3	266.9	−35.8
	216	224.5	−9.2	251.4	267.8	−36.0

tion of isothermal crystallization at various T_c values, and the melting parameters are summarized in Table III. The DSC heating curves of these specimens contain three melting peaks. Apparently, peak I is present in all samples at a temperature (ca. 225.0°C) close to the melting peak of the pure PTT component. According to the position and height of peak I, it can be supposed that peak I corresponds to the melting of the crystals of the PTT component. Both peak II and peak III present at higher temperatures (ca. 248.1–255.0°C for peak II and 265.8–267.8°C for peak III), and this can be explained according to Lin and Koernig.[29] We think that the lower temperature melting peak (peak II) corresponds to small and/or imperfect crystals of the PEN component, whereas the higher melting peak (peak III) results from the melting of the perfect crystals formed near the isothermal T_c. According to careful observation, with increasing T_c, peak II shifts to a higher temperature, and this indicates that the crystals that form at higher T_c's become larger and more perfect than those formed at lower T_c's. In a comparison of B2 and B3 crystallized at 214 and 216°C, all three peaks of B2 are higher for T_m than those of the B3 sample. The total melting enthalpy ($\Delta H_{f(II+III)}$) is calculated from the beginning of the melting of peak II to the end of the melting of peak III. $\Delta H_{f(II+III)}$ of B3 is higher than that of the B2 blend at the same T_c, and this also indicates that the PTT component can improve the crystallization ability of the PEN component.

According to careful observation, the melting peak temperatures (peak I) near 225°C in Figure 6(a,b), which are ascribed to the melting of PTT, as well as the melting enthalpy ($\Delta H_{f(I)}$) in Table III, are a little smaller for B3 (40% PTT) than for B2 (20% PTT) at the same T_c. Because the crystallization rate of B3 is higher than that of B2 at the same T_c (214 and 216°C) during the isothermal-crystallization process, the crystal perfection and crystallinity of PTT in the B3 blend are worse and lower than those in B2. The worse perfect crystallites and lower crystallinity component will melt at a lower temperature and with lower melting enthalpy, so peak I of B3 can be observed at a lower temperature with a lower melting enthalpy in the DSC melting curve in comparison with B2.

Crystallization activation energy (ΔE)

The crystallization process of the B2 and B3 blends is assumed to be thermally activated. K_t can be approximately described by the following Arrhenius equation:[30]

$$K_t^{1/n} = K_0 \exp(-\Delta E/RT_c) \tag{4}$$

$$(1/n)\ln K_t = \ln K_0 - \Delta E/RT_c \tag{5}$$

where K_0 is the temperature-independent pre-exponential factor and R is the gas constant. ΔE can be determined from the slope coefficient of plots of $(1/n)\ln K_t$ versus $1/T_c$ in eq. (5), which is shown in Figure 7.

In this case, the ΔE values for the B2 and B3 blends are −48.3 and −60.9 kJ/mol, respectively. ΔE of the B3 blend is more negative than that of the B2 blend.

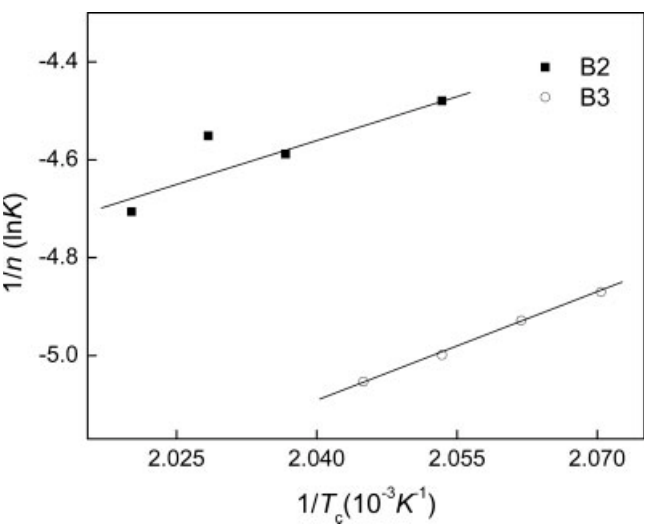

Figure 7 Plot of $1/n(\ln K)$ versus $1/T_c$ from the Arrhenius method for the isothermal-crystallization activation energy of the B2 and B3 blends.

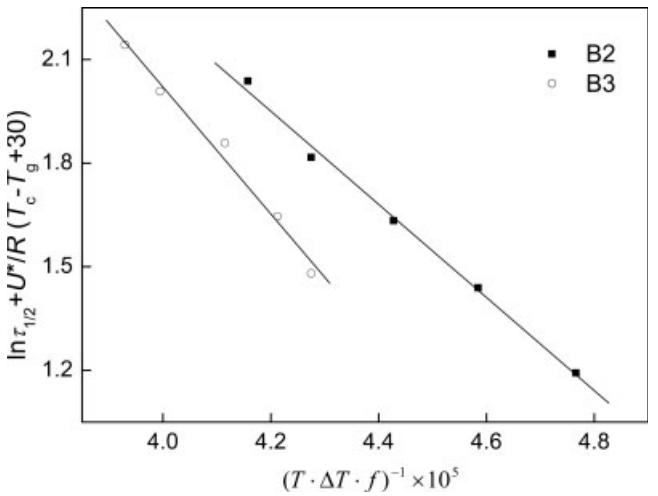

Figure 8 Plot of eq. (8) for the B2 and B3 blends.

Generally, the smaller ΔE is, the higher the probability is of the molten fluid transforming into the crystalline state.[31–33] This result suggests that ΔE of the blends decreases as the PTT content increases, indicating that an increasing amount of the PTT component can improve the crystallization ability of the PEN component.

Hoffman–Lauritzen theory analysis

According to the Hoffman–Lauritzen theory,[34] the dependence of the growth rate of the spherulite (G) on the temperature (T) can be described as follows:

$$G = G_0 \exp\left[\frac{-U^*}{R(T_c - T_\infty)}\right] \exp\left[\frac{-K_g}{T_c(\Delta T)f}\right] \qquad (6)$$

where G_0 is the pre-exponential factor and U^* is the activation energy of the segmental jump. U^* is different from ΔE derived from the Arrhenius equation, which is the apparent activation energy of K_t. $\Delta T = T_m^0 - T_c$ is the degree of undercooling, $f = 2T_c/(T_m^0 + T_c)$ is the correction factor, T_m^0 is the equilibrium melting temperature, and $T_\infty = T_g - 30$ K is a hypothetical temperature at which motion associated with viscous flow ceases and that is usually taken to be 30 K below T_g.[34] K_g is a kinetic parameter. By rearranging eq. (6)

$$\ln G + \frac{U^*}{R(T_c - T_\infty)} = \ln G_0 - \frac{K_g}{T_c(\Delta T)f} \qquad (7)$$

we can determine K_g from the linear plot of the left-hand side of eq. (7) versus $(T_c\Delta Tf)^{-1}$. U^* is typically taken as the universal value of 6.3 kJ/mol.[34] To make eq. (7) suitable for isothermal DSC data, Chan and Isave[35] proposed an empirical modification that replaces the growth rate with the reciprocal time ($\tau_{1/2} = 1/t_{1/2}$) to reach half of X_t:

$$\ln \tau_{1/2} + \frac{U^*}{R(T_c - T_\infty)} = \ln G_0 - \frac{K_g}{T_c(\Delta T)f} \qquad (8)$$

In this article, $U^* = 6.3$ kJ/mol is applied to achieve a very good fit to the plot of $\ln \tau_{1/2} + U^*/R(T_c - T_\infty)$ versus $(T_c\Delta Tf)^{-1}$, as shown in Figure 8, and the kinetic parameters are listed in Table IV. The regime transitions cannot be clearly observed for B2 and B3. The reason for this might be that the temperature range used for the isothermal crystallization of these samples is much narrower, and thus the whole regime range is not achieved. T_c is much lower for the crystallization of B2 and B3 blends in this article, so the value of n may be 2 (in regime ii). According to Table IV, the values of K_g are 1.5×10^5 K^2 for B2 and 1.8×10^5 K^2 for B3, and they are consistent with Lee et al.'s study.[36] The B2 blend has a higher K_g value than B3, and this suggests that the crystallization process of PEN is improved by the addition of PTT; the result agrees with the previous Avrami results.

K_g has the following form:

$$K_g = \frac{nb_0\sigma\sigma_e T_m^0}{\Delta h_f k_B} \qquad (9)$$

where σ and σ_e are the lateral and fold surface free energies, respectively, of the growing crystal and b_0 is the molecular layer thickness (0.566 nm).[36] According to Wu and Liu,[37] T_m^0 for PEN (β form) ranges from 282 to 292°C; we have chosen this value over a slightly larger one (297°C). Δh_f is the heat of fusion per unit of volume of the crystal (2.67×10^8 J/m^3),[36] k_B is the Boltzmann constant, and n takes the value of 4 for crystallization regimes i (at higher T_c) and iii and 2 for regime ii (at lower T_c).

σ can be calculated by an empirical equation[38] as follows:

$$\sigma = \alpha(\Delta h_f)(a_0 b_0)^{1/2} \qquad (10)$$

TABLE IV
Values of K_g, σ_e, and σ for the B2 and B3 Blends in Regime ii

Sample	T_g (K)	T_m^0 (K)	a_0 (nm)	b_0 (nm)	U^* (kJ/mol)	K_g (10^{-5} K^2)	σ (10^{-2} J m^2)	$\sigma\sigma_e$ (10^{-4} J^2 m^4)	σ_e (10^{-2} J m^2)	r^2
B2	367	570	0.651	0.566	6.3	1.5	1.78	8.58	4.80	99.7
B3	355	570	0.651	0.566	6.3	1.8	1.78	10.3	5.77	99.2

where a is derived empirically to be 0.11. Parameters a_0 and b_0 are the monomolecular width and layer thickness, and their values are 0.651 and 0.566 nm,[36] respectively. All the parameters and results are also listed in Table IV. It is well known that the greater σ_e is with respect to σ, the more fibrous the shape will be of the nucleus.[39] As shown in Table IV, the value of σ_e with respect to the σ value of B3 is greater than that of the B2 blend, indicating that the nucleus shape of B3 is more fibrous than that of the B2 blend.

Spherulitic morphology

After 3 h of annealing at 190°C, the crystallization morphology of blends B1–B6 was observed with POM, and six images were obtained, as shown in Figure 9. Within the volume between the two glass plates with a distance of about 200 μm, many small Maltese crosses (20–60 μm in size) can be observed, and all the samples show a relatively well-defined spherulitic texture with clear Maltese crosses, except for B1 and B2. For B1 and B2, the dimensions and degree of perfection of the spherulites are less than those of B3–B6. For pure PTT (B6), the dimensions and perfection of the spherulites are the best among all the samples. This suggests that PTT with flexible molecular chains is more crystallizable than PEN with chain stiffness. In addition, with an increasing concentration of the PTT component in the blends, the Maltese crosses become more and more clear, and the spherulites increase in size from 20 to 80 μm gradually. These results indicate that the PTT component in the blends

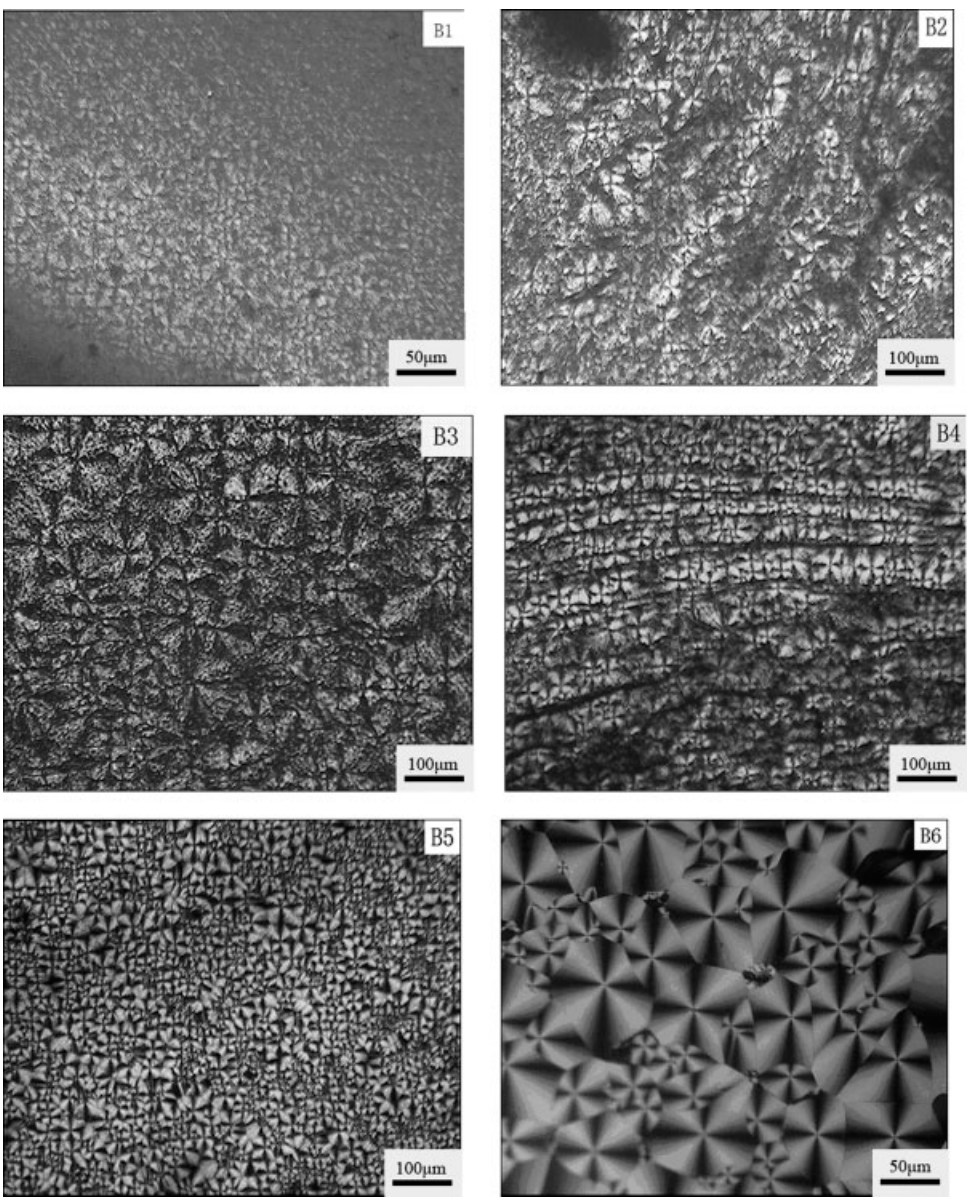

Figure 9 Polarized optical micrographs of PTT/PEN blends at 190°C.

improves spherulite growth and forms perfect spherulites in blends.

CONCLUSIONS

In PTT/PEN binary blends, the PTT component is a diluent for PEN and improves the mobility of its molecular chains and its crystallization ability. The binary blends show different crystallization behaviors with various contents of PTT in them. When the PTT concentration is less than 50 wt %, the crystallization of the PTT component is inhibited by the major component, PEN, whereas the crystallization behavior of PEN is improved by PTT. When the PTT concentration is increased to more than 50 wt %, both the PTT and PEN components in the blends crystallize individually. The Avrami analysis of the isothermal-crystallization process of B2 and B3 shows primary and second stages. In the primary stage, n is in the range of 3.0–3.3, and the crystal nucleation type may include both thermal and athermal nucleation; the growth dimension should predominantly be three-dimensional. The crystallization rates of the PEN component in the binary blends increase with an increasing concentration of PTT, whereas ΔE decreases with increasing PTT. The observation of subsequent melting endotherms of the blends after isothermal crystallization at the specified T_c values show multiple melting peaks: the lower one corresponding to the melting endotherm of PTT, the middle one corresponding to the melting of the smaller and unperfected crystallites of PEN, and the higher one corresponding to the melting of the perfect crystals of PEN. Finally, the Hoffman–Lauritzen theory has also been employed to fit the process of isothermal crystallization, and kinetic parameters K_g, σ, and σ_e of the samples with 20 or 40 wt % PTT have been determined. The spherulite morphologies of the six binary blends that form at 190°C show different sizes and perfect Maltese crosses when the PTT or PEN component is varied, and this suggests that the more PTT there is, the larger or more perfect the crystallites are that form in the binary blends.

References

1. Whinfield, J. R.; Dickson, J. T. Brit Pat 578,079 (1946).
2. Wu, J.; Schultz, J. M.; Samon, J. M.; Pangelinan, A. B.; Chuah, H. H. Polymer 2001, 42, 7141.
3. Ramiro, J.; Eguiazábal, J. I.; Nazábal, J. Polym Adv Technol 2003, 14, 129.
4. Nakamae, K.; Nishino, T.; Tada, K.; Kannamoto, T.; Ito, M. Polymer 1993, 34, 3322.
5. Van Den Heuvel, C. J. M.; Klop, E. A. Polymer 2000, 41, 4249.
6. Gao, X.; Hou, W.; Zhou, J.; Li, L.; Zhao, L. Macromol Mater Eng 2004, 289, 174.
7. Yao, Z.; Zhu, C. C.; Cheng, M.; Liu, J. Comput Mater Sci 2001, 22, 180.
8. Yu, M. F.; Files, B. S.; Arepalli, S.; Ruoff, R. S. Phys Rev Lett 2000, 84, 5552.
9. Yoon, K. H.; Lee, S. C.; Park, O. O. Polym Eng Sci 1995, 35, 1807.
10. Yu, Y.; Choi, K. J. Polym Eng Sci 1997, 37, 91.
11. Supaphol, P.; Dangseeyun, N.; Thanomkiat, P.; Nithitanakul, M. J Polym Sci Part B: Polym Phys 2004, 42, 676.
12. Dangseeyun, N.; Supaphol, P.; Nithitanakul, M. Polym Test 2004, 23, 187.
13. Rwei, S. P. Polym Eng Sci 1999, 39, 2475.
14. Krutphun, P.; Supaphol, P. Eur Polym J 2005, 41, 1561.
15. Allan, R. M.; John, J. L. J Appl Polym Sci 2004, 92, 2791.
16. Ho, J. C.; Lin, T. C.; Wei, K. H. Polymer 2000, 41, 9299.
17. Penning, J. P.; Manley, R. Macromolecules 1996, 29, 77.
18. Xing, P.; Ai, X.; Dong, L.; Feng, Z. Macromolecules 1998, 31, 6898.
19. Shi, Y.; Jabarin, S. A. J Appl Polym Sci 2001, 81, 11.
20. Avrami, M. J Chem Phys 1940, 8, 212.
21. Avrami, M. J Chem Phys 1936, 7, 1103.
22. Wunderlich, B. Macromolecular Physics; Academic: New York, 1976; Vol. 2.
23. Pérez-Ćardenas, F. C.; Del Castillo, L. F.; Vera-Graziano, R. J Appl Polym Sci 1991, 43, 779.
24. Liu, S.; Yu, Y.; Cui, Y.; Zhang, H.; Mo, Z. J Appl Polym Sci 1998, 70, 2371.
25. Janeschitz-Kriegl, H.; Ratajski, E.; Wipel, H. Colloid Polym Sci 1999, 227, 217.
26. Xue, M. L.; Sheng, J.; Yu, Y. L.; Chuah, H. H. Eur Polym J 2004, 40, 811.
27. Supaphol, P. Thermochim Acta 2001, 370, 37.
28. Supaphol, P.; Spruiell, J. E. J Macromol Sci Phys 2000, 39, 257.
29. Lin, S. B.; Koernig, J. L. J Polym Sci Polym Symp 1984, 71, 121.
30. Cebe, P.; Hong, S. D. Polymer 1986, 27, 1183.
31. Run, M. T.; Wu, S. Z.; Zhang, D. Y.; Wu, G. Polymer 2005, 46, 5308.
32. Dangseeyun, N.; Supaphol, P.; Nithitanakul, M. Polym Test 2004, 23, 175.
33. Vyazovkin, S.; Dranca, I. Macromol Chem Phys 2006, 207, 20.
34. Hoffman, J. D.; Davis, G. T.; Lauritzen, J. I. Jr. In Treatise on Solid State Chemistry; Hannay, N. B., Ed.; Plenum: New York, 1976; Vol. 3, p 479.
35. Chan, T. W.; Isaev, A. I. Polym Eng Sci 1994, 34, 461.
36. Lee, W. D.; Yoo, E. S.; Im, S. S. Polymer 2003, 44, 6617.
37. Wu, T. M.; Liu, C. Y. Polymer 2005, 46, 5621.
38. Lauritzen, J. I., Jr.; Hoffman, J. D. J Appl Phys 1973, 44, 4340.
39. Wunderlich, B. Macromolecular Physics: Crystal Nucleation, Growth, Annealing; Academic: New York, 1976; Vol. 3.